Oracle bone script records explain the impact of climate extremes in ancient China

Siyang Li[1]†, Ke Ding[2,3,4]†, Aijun Ding[2,3]*, Shiyan Zhang[1], Xin Huang[2,3,4], Sijia Lou[2,3,4], Derong Zhou[2,3], Lejun He[5], Xiaolu Zhou[5], Zhe-Min Tan[2,3], Congbin Fu[2,3], Quansheng Ge[1,3]*

[1]Institute of Geographic Sciences and Natural Resources Research, Chinese Academy of Science; Beijing 100101, China

[2]School of Atmospheric Sciences, Nanjing University; Nanjing 210023, China

[3]Jiangsu Provincial Innovation Center for Climate Change; Nanjing 210023, China

[4]Frontiers Science Center for Critical Earth Material Cycling, Nanjing University; Nanjing 210023, China

[5]School of History, Nanjing University; Nanjing 210023, China

*Corresponding author. Email: geqs@igsnrr.ac.cn (Q.G.); dingaj@nju.edu.cn (A.D.)

†These authors contributed equally to this work.

Abstract: Extreme climatic and weather events have raised increasing concerns in the context of climate change for causing severe disasters worldwide. As for ancient civilizations, however, possible causes of extreme events and their corresponding cultural responses have remained unclear. By quantitatively analyzing the weather information in ~55000 oracle bone script pieces, we constructed three ~200-year indexes representing drought, flood and rainfall conditions in the Chinese Bronze Age. Combined with paleoclimatic proxies, meteorological data, model simulations, and archaeological evidence, here we find that millennial-scale strong El Niño and typhoon activities caused extreme droughts and floods in the central plains of China, thus notably influencing early cultures and civilizations in China.

1.Introduction

The great impact of climate change on ancient cultures and civilizations has been examined and reported worldwide (*1-3*). As China is a country with a long history, previous studies have established that Chinese civilization has long been affected by past climatic fluctuations in various aspects (*4*). Among all climate change-related factors, centennial-scale fluctuations in air temperature and monsoon precipitation have been considered crucial as they created favorable or challenging climatic and environmental conditions in East Asia for peoples' survival and cultural development (*4*). Remarkably, climate change-induced extreme events, often accompanied by natural weather disasters, can also pose a severe threat to human civilization (*5-7*). However, while societal and cultural responses to variations in climatic averages have been widely addressed, the impact of catastrophic weather events on ancient peoples and their civilizations remains unclear, especially in earlier times when literature records are relatively lacking.

The earliest form of systematic Chinese writing—oracle bone scripts—provides valuable information about the civilization of the Shang dynasty in the Chinese Bronze Age (*8*). By quantitatively studying the inscriptions related to weather for ~200 years since 3200 BP (*9*), we examined the extent to which the Shang people were concerned about rainfall and its related disasters, and then investigated the linkage between people's weather concerns and the fluctuations in El Niño and typhoon activities based on paleoclimatic proxies. By combining modern meteorological analysis, model simulations, and archaeological evidence, we attempt to clarify how climate change, in the millennial scales, induces devastating events on the central plains of China, thus offering new insight into how past climate extremes influenced human civilization in ancient times.

2. Cultural evolution and climate background

The central plains of China have been regarded as the "Cradle of Chinese civilization" (*10*). Dating from approximately 6000 BP to 3000 BP, the early cultural centers (ECCs) that belonged to different archaeological periods in central China were mainly located along the middle and lower reaches of the ancient Yellow River (Fig. 1A) (*11*). As shown in Fig. 1, during different periods, these ECCs moved among cities, e.g., Sanmenxia, Luoyang, Zhengzhou, and Anyang, along the Yellow River at a millennial scale. Accordingly, demographic curves in Luoyang and Zhengzhou (data got in Yiluo (*12*) and Dahecun (*13*)) also showed strong millennial-scale fluctuations (Fig. 1B), indicating a possible impact of periodic climate change.

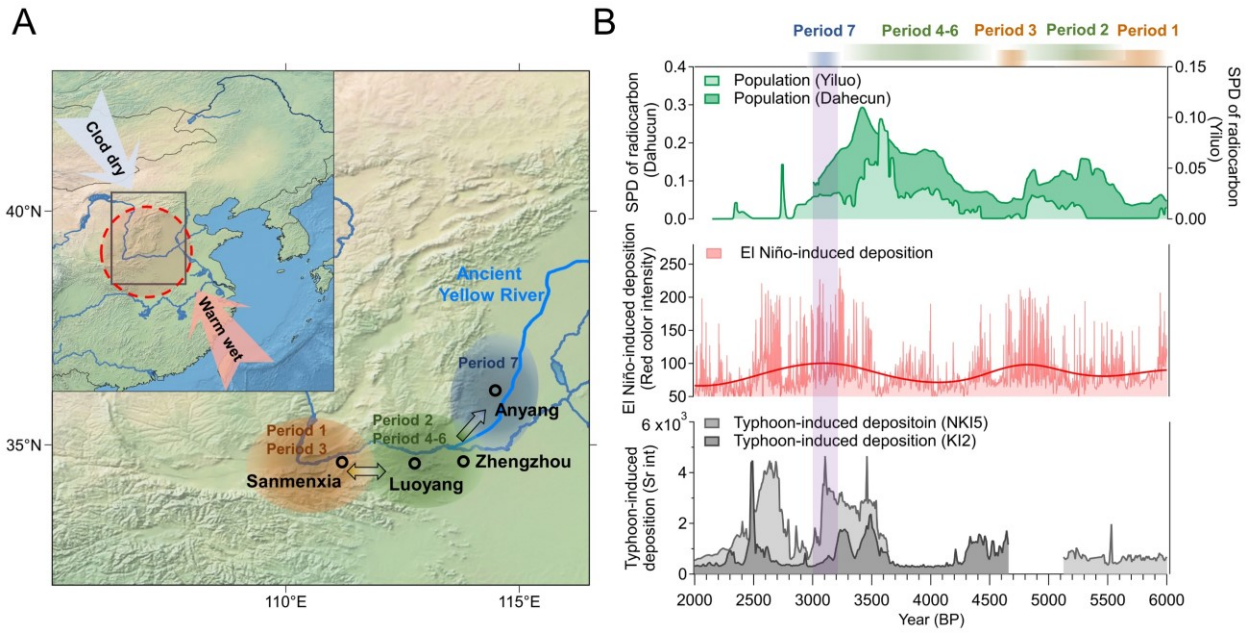

Fig. 1. Early demographic fluctuation and cultural center movement (~6000-3000 BP) in the central plains of China with corresponding El Niño and typhoon variations. (**A**) The shaded areas (brown, green and blue) show the varied locations of cultural and civilization centers in central China in different periods (Periods 1-7, table S1) (*9, 12*). The white and red arrows in the upper-left corner of the map represent cold–dry and warm–wet air, respectively; the grey box denotes the region of the enlarged map in panel (A); and the red circle represents the approximate central region of early cultures and civilizations in central China (*10*). (**B**) Variations in population size in the Luoyang and Zhengzhou areas on the central plains of China, as represented by the time series of the Summed Probability Distribution (SPD) of radiocarbon databases in the Yiluo region

(*12*) and at the Dahecun site (*13*); variations in El Niño-induced sediments in southern Ecuador (*19*) and typhoon-induced sediments in southwestern Japan (*20*). The solid red line indicates the El Niño trend calculated by 1000-year ensemble empirical mode decomposition (EEMD) filter smoothing. In addition, the colors of the stripes above the top axis (corresponding to the colors of the shaded areas in panel (A)) represent the locations of cultural and civilization centers in different periods. The purple shaded area denotes the time span of the oracle bone scripts.

Monsoons have been considered one of the main factors influencing cultures and civilizations in China (*14-16*). However, all identified ECCs (~200 km away from each other) are located in the summer monsoon area, nearly one thousand kilometers away from the monsoon's northern edge. Changes in the monsoon onset cannot explain these ECCs' movement over such a small distance. In fact, the average air temperature and moisture conditions, which are strongly affected by monsoons, did not appear to be the dominant factors affecting cultural evolution in these times (fig. S1) (*17, 18*). Remarkably, the population change showed good linkage with millennial-scale El Niño (*19*) and typhoon fluctuations (*20*) (Fig. 1B). The population strongly decreased during periods with strong El Niño and typhoon signals, e.g., from 3500-3000 BP and 5300-4700 BP, while opposing trends existed in periods with weak El Niño and typhoon signals, e.g., from 6000-5300 BP and 4700-3500 BP.

3. Climate extremes recorded in oracle bone scripts

Oracle bone scripts, as divinations of royalty and nobility, are considered the earliest form of systematic Chinese writing ever discovered (*8*). Since the late 19th century, tens of thousands of oracle bones have been found in Anyang (Fig. 1A, shaded in blue) and have been identified as invaluable cultural relics and contemporary documentation of the Late Shang dynasty (*9*).

Remarkably, the ~200-year time span (3200-2996 BP) over which these divinations were recorded belonged to a typical period characterized by strong El Niño and typhoon activities together with a simultaneous population decline in the central plains of China (Fig. 1B). Moreover, several character patterns of oracle bone scripts suggest an enormous influence of floods and droughts at that time. For example, a water-wave-like pattern is one of the main "disaster" characters, and a locust-like pattern can represent both locust plagues (always accompanying heavy droughts (*21*)) and the autumn season (*22*) (Fig. 2A). Therefore, we collected and examined ~55000 pieces of oracle bone scripts (table S2) and built up three major indexes representing flood, drought and rainfall variations during these ~200 years in the Late Shang dynasty. These three indexes were constructed from the proportions of pieces that contained "flood", "pray for rain", and "rainfall condition" in the five oracle bone script phases (Fig. 2B, fig. S2 and tables S3 and S4, Materials and Methods). As can be seen from Fig. 2, C and D, all three indexes show notable fluctuations across the ~200 years of record, suggesting drastic changes in meteorological conditions and related disasters in the Late Shang dynasty.

First, the notable variation in drought conditions identified based on the reconstructed drought index can be supported by the similar fluctuations in locust plagues (*22*) and archaeological-based ground water levels (*23*) (Fig. 2C and fig. S3). Interestingly, the drought index shows a very good correlation with the El Niño proxy retrieved by Moy et al. (*19*), with the highest values occurring in the high El Niño phase 4, implying an impact of El Niño on severe droughts. These results suggest that the rainfall changes that occurred on the central plains of China during the Late Shang dynasty were mainly affected by the El Niño–Southern Oscillation (ENSO) (*24*). In fact, modern

meteorological data also supports that droughts on the central plains of China are associated with strong El Niño events. For example, the strong El Niño events that occurred during 1982-1983, 1997-1998, and 2015-2016 decreased summer rainfall in northern China by 20%-40% by causing a north wind anomaly that reduced the water vapor supply (fig. S4) (*24-27*). Given the greater intensity and frequency of strong El Niño events from 3600 BP to 3000 BP (*19*), much heavier droughts and more locust plagues would have occurred in the Shang dynasty, and these events were recorded in oracle bone scripts by the Shang people themselves.

Regarding the flood situation, the flood index also shows strong fluctuations during the five phases across these ~200 years (Fig. 2D). Surprisingly, the flood and drought indexes increased simultaneously in several phases, e.g., in phases 1 and 4. This contradictory result may be explained that increased floodwaters may not have been caused by a change in average rainfall but rather from extreme rainfall events (*28*). Furthermore, due to soil erosion caused by El Niño-induced droughts, extreme rainfall could not ease drought conditions but, on the contrary, brought much more severe floods (*29*).

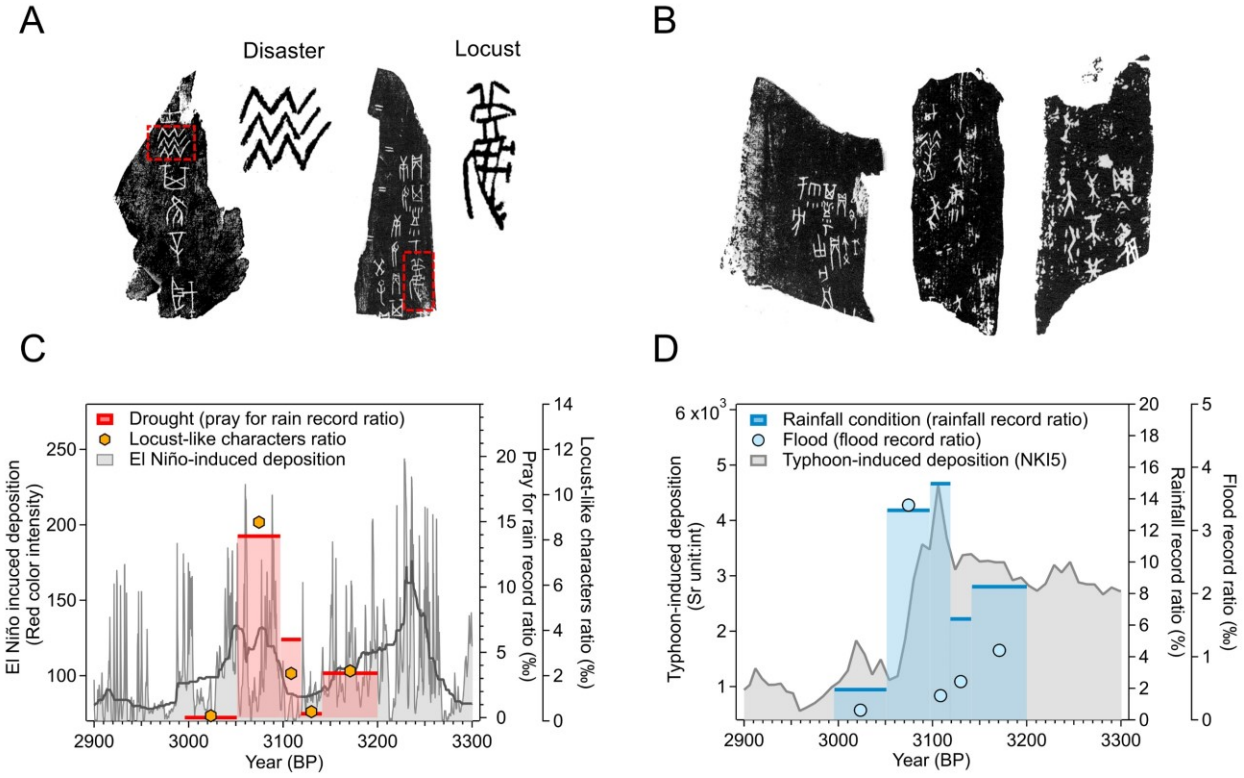

Fig. 2. Flood and drought conditions in the Late Shang oracle bone script divinations. (**A**) Rubbings of oracle bones or tortoise shells (from *Oracle Bone Script Complications*, table S2). Left: piece No. 12836, "Will there be a disaster? ……". Right: piece No. 33234, "Divination in the day of Gengchen: Shall we pray to (some god) for ending the locust plague? ……". In addition, the "disaster" and "locust" characters, highlighted by red boxes, are shown beside the rubbings. (**B**) Typical rubbing examples that contain the symbols for "rain", "praying for rain" and "flood" (from *Oracle Bone Script Complications*, table S2). Left to right: piece Nos. 32992, 34226, and 33351. The translation of these three pieces are presented in fig. S2. (**C**) Variations in the drought index (the "pray for rain" record ratio), proportion of locust-like characters and El Niño-caused sediments (the solid grey line denotes the 100-point running average) (*19*). The different widths of the red bars represent the time range of each oracle bone script phase. (**D**) Similar to panel (C)

but representing the variations in the flood index (flood record ratio), rainfall condition index (rainfall record ratio) and typhoon-caused sediments in southwestern Japan (marked as a black circle in Fig. 3B) (*20*).

3. Extreme floods caused by typhoons

Extreme rainfall on the central plains of China is often associated with Pacific typhoon activities in the present day (*30, 31*). Similarly, as shown in Fig. 2D, the reconstructed rainfall index in the Late Shang dynasty also shows simultaneous changes with typhoon-induced sediments in southwestern Japan (location shown in Fig. 3B); these sediment records mainly indicate northward typhoon activities over the past 6500 years (*20*).

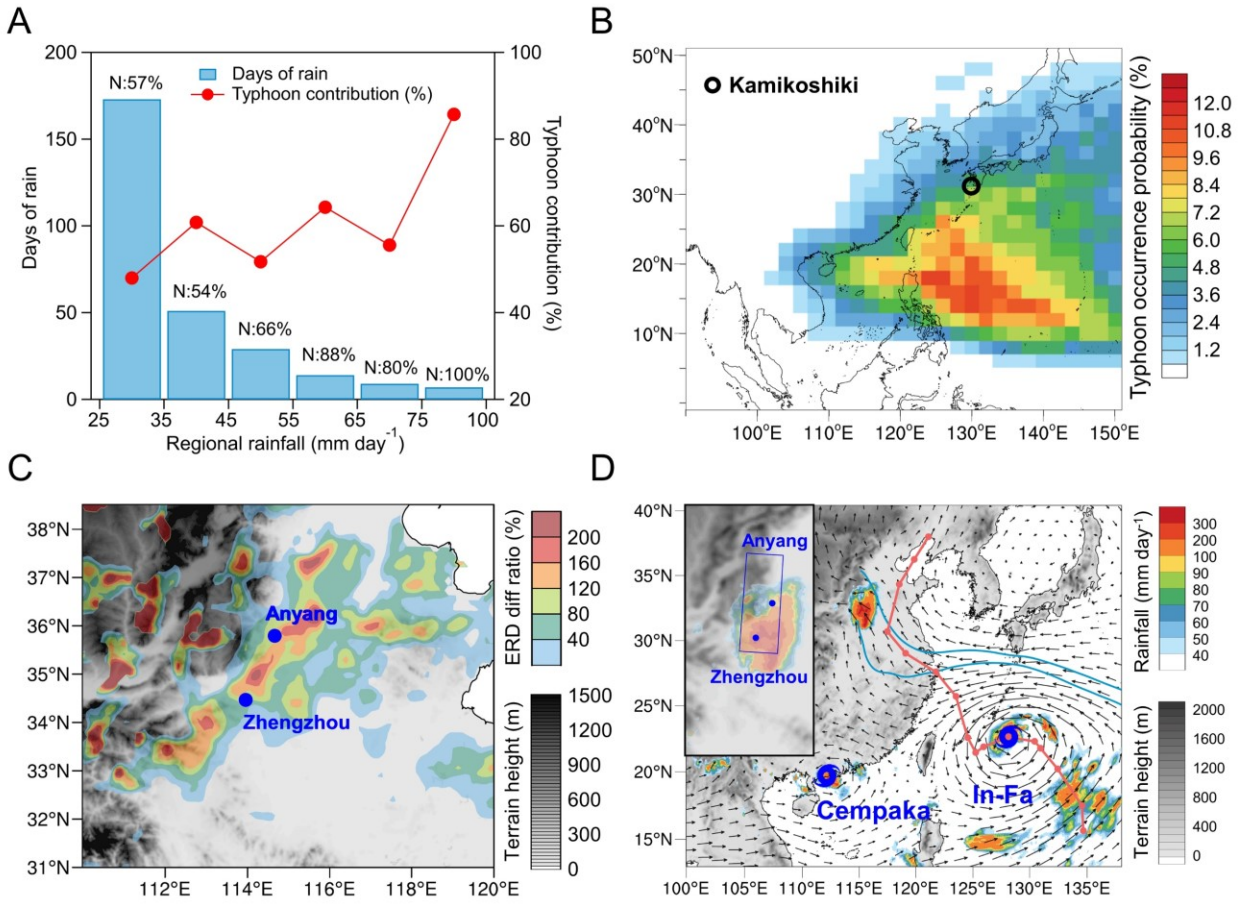

Fig. 3. Typhoon influences on rainfall on the central plains of China. (**A**) Regional daily rainfall frequency distribution and typhoon contribution ratio in Zhengzhou, Anyang and the surrounding area (shown in panel (D) with the blue box) from 1950 to 2021. The ratio of northward typhoons is shown with "N:" as the prefix. (**B**) Probability of a typhoon passing through each grid from 1950 to 2021. The black circle gives the location where the typhoon-induced sediment data was got. (**C**) Increased ratio of the extreme rainfall day (ERD) number in the upper-quartile years with the most northward typhoons. (**D**) Typhoons In-Fa and Cempaka and the induced extreme rainfall (data from the Integrated Multi-satellite Retrievals for Global Precipitation Measurement (IMERG)) on 20 July 2021. The vectors denote the wind field at 850 hPa. The light blue lines show the streamlines at the southern and northern boundaries of the Zhengzhou and Anyang areas. The red line provides the track of Typhoon In-Fa, with the markers indicating the typhoon centers' location at 12 UTC each day. The small picture in the upper-left corner is an enlarged view of the topography and rainfall distribution.

According to the reanalysis data of the past 70 years, northward typhoons contributed more than 85% of rainy days when the regional daily rainfall exceeded 75 mm/day (6 out of the 7 cases were affected by typhoons; see the Materials and Methods section) on the central plains of China (Fig. 3A). The eastern slopes of mountains even suffered from more than 100% increases in extreme rainfall days (greater than 100 mm/day) in the upper-quartile years with the most northward typhoons (Fig. 3C). Northward typhoons often cause extreme rainfall and flood disasters under the interaction of water vapor advection and topography (*30-33*) (fig. S5). The "7.21" rainstorm (2021) that occurred in Zhengzhou, which shocked the whole country, is a typical example showing how typhoon activities can cause catastrophic rainstorms and floods in this region (Fig. 3D). Under the influence of Typhoons In-Fa and Cempaka, disastrous rainstorms with 24-hour rainfall totals exceeding 500 mm caused severe floods, landslides and enormous losses in Zhengzhou and neighboring cities on 20 July 2021 (*34, 35*). Similarly, historically high-impact floods (e.g., the floods of August 1975 and August 1996) have also been found to be related to typhoon activities (*30, 31*) (fig. S5). Numerical sensitivity simulations performed at different typhoon intensities also demonstrated important impacts of typhoons on extreme rainfall on the central plains of China (*36*) (fig. S6, Materials and Methods).

Based on the mechanism described above, the consistency of the reconstructed rainfall index and typhoon-induced sediment record during the Late Shang dynasty implies that increased typhoon activities caused more extreme rainfall events on the central plains of China at that time. A similar concurrence of increased typhoon activities and flood disasters can also be found during the 500-1200 BP period (fig. S7) (*37, 38*), as supported by other literature-based records (*39*).

4. Discussions on the evolution of civilization in ancient China

The above results show that millennial-scale strong El Niño and typhoon activities brought extreme droughts and floods to the central plains of China, and these events were recorded in the divinations of oracle bone scripts during the Late Shang dynasty. Such conclusions can also be supported by the evidence of floods on city walls (*40*), the migration of settlements to upper-river regions (*41, 42*), and the improved drainage systems recorded in archaeological data (*43, 44*) in the Shang dynasty. Over longer time scales, millennial-scale extreme events could explain the changes in population and the movements of ECCs in the central plains of China from 6000 BP to 3000 BP. During strong El Niño and typhoon periods, the population in the alluvial plain or basin (green area in Fig. 1A) declined, and the ECCs tended to leave this region to move westwards into mountainous areas (brown area in Fig. 1A) or northwards to the piedmont slopes (blue area in Fig. 1A) to ease the vast losses resulting from flood disasters. From the point of view of cultural development, millennial-scale fluctuations in El Niño and typhoon events can even exert an influence on the evolution of cultures and civilizations in central China, for the two major periods of great development, which are characterized by the building of the first vast cities, class differentiation and widespread Monarchy country (*9, 45*), were both concurrent with the weak El Niño and typhoon periods that occurred during 6000-3000 BP.

Based on oracle bone script records, paleoclimate proxies and modern meteorological data, our results extend the knowledge of human responses to past climate change by pointing out the significant impacts of extreme events induced by millennial-scale fluctuations in El Niño and typhoon activities. With the future discovery of more literature records and archaeological evidence, we may gain more insights into how past climate extremes influenced the evolution of

ancient civilizations in widespread global areas (*1, 7*). Even today, El Niño and typhoon/hurricane activities are among the main concerns at various time scales (*16, 46*). Considering the increasing likelihood of more frequent devastating ENSO and typhoon extremes in the context of global warming (*46, 47*), this finding can help us better prepare for the changing climate (*48, 49*), especially in inland developing countries and regions.

References

1. H. Weiss, R. S. Bradley, What Drives Societal Collapse? *Science* **291**, 609-610 (2001).
2. P. B. deMenocal, Cultural responses to climate change during the Late Holocene. *Science* **292**, 667-673 (2001).
3. D. D. Zhang, P. Brecke, H. F. Lee, Y.-Q. He, J. Zhang, Global climate change, war, and population decline in recent human history. *Proc. Natl. Acad. Sci. U. S. A.* **104**, 19214-19219 (2007).
4. Q. Ge, H. Liu, J. Zheng, L. Xiao, The climate change and social development over the last two millennia in China. *Chinese Journal of Nature* **35**, 9-21 (2013).
5. Z. Xia, Z. Wang, Q. Zhao, Extreme flood events and climate change around 3500 aBP in the Central Plains of China. *Sci. China Ser. D-Earth Sci.* **47**, 599 (2004).
6. H. Zhang *et al.*, Collapse of the Liangzhu and other Neolithic cultures in the lower Yangtze region in response to climate change. *Sci. Adv.* **7**, eabi9275 (2021).
7. R. Grove, G. Adamson, *El Niño in world history*. (Springer, 2018).
8. K.-c. Chang, *Shang Civilization*. (Yale University Press, New Haven, Connecticut, 1980).
9. X. S. Z. C. P. Team, *Research Report of Xia Shang Zhou Chronology Project*. (Science Press, Beijing, 2022), pp. 186-249, 324-359. (in Chinese)
10. W. Yan, The unity and diversity of prehistoric cultures in China. *Cultural Relics* **3**, 38-50 (1987). (in Chinese)
11. L. Liu, X. Chen, *The Archaeology of China: From the Late Paleolithic to the Early Bronze Age*. (Cambridge University Press, New York, NY, 2012).
12. L. Liu *et al.*, Rise and fall of complex societies in the Yiluo region, North China: The spatial and temporal changes. *Quat. Int.* **521**, 4-15 (2019).
13. X. Ren *et al.*, Holocene fluctuations in vegetation and human population demonstrate social resilience in the prehistory of the Central Plains of China. *Environ. Res. Lett.* **16**, 055030 (2021).
14. F. Chen *et al.*, Westerlies Asia and monsoonal Asia: Spatiotemporal differences in climate change and possible mechanisms on decadal to sub-orbital timescales. *Earth-Sci. Rev.* **192**, 337-354 (2019).
15. P. Zhang *et al.*, A Test of Climate, Sun, and Culture Relationships from an 1810-Year Chinese Cave Record. *Science* **322**, 940-942 (2008).
16. D. Xu *et al.*, Synchronous 500-year oscillations of monsoon climate and human activity in Northeast Asia. *Nat. Commun.* **10**, 4105 (2019).

17. Q. Pei, D. D. Zhang, J. Li, H. F. Lee, Proxy-based Northern Hemisphere temperature reconstruction for the mid-to-late Holocene. *Theor. Appl. Climatol.* **130**, 1043-1053 (2017).

18. X. Fang, G. Hou, Synthetically reconstructed Holocene temperature change in China. *Scientia Geographica Sinica* **31**, 385-393 (2011).

19. C. M. Moy, G. O. Seltzer, D. T. Rodbell, D. M. Anderson, Variability of El Nino/Southern Oscillation activity at millennial timescales during the Holocene epoch. *Nature* **420**, 162-165 (2002).

20. J. D. Woodruff, J. P. Donnelly, A. Okusu, Exploring typhoon variability over the mid-to-late Holocene: evidence of extreme coastal flooding from Kamikoshiki, Japan. *Quat. Sci. Rev.* **28**, 1774-1785 (2009).

21. X. Guo *et al.*, 4-Vinylanisole is an aggregation pheromone in locusts. *Nature* **584**, 584-588 (2020).

22. X. Yao, D. Xiao, *Collection and Classification of Inscriptions on Bones and Tortoise Shells in Yinxu*. (China Book Company, Beijing 1989), pp. 484-485, 694-696. (in Chinese)

23. W. Zhou, Exploration of the climatic conditions in Yinxu during the Late Shang period. *Journal of Chinese Historical Geography* **1**, 185-196 (1999). (in Chinese)

24. B. Wang, J. Li, Q. He, Variable and robust East Asian monsoon rainfall response to El Nio over the past 60 years (1957-2016). *Adv. Atmos. Sci.* **34**, 1235-1248 (2017).

25. F. Ma, A. Ye, J. You, Q. Duan, 2015-16 floods and droughts in China, and its response to the strong El Nino. *Sci. Total Environ.* **627**, 1473-1484 (2018).

26. K.-M. Lau, H. Weng, Coherent modes of global SST and summer rainfall over China: An assessment of the regional impacts of the 1997-98 El Nino. *J. Clim.* **14**, 1294-1308 (2001).

27. R. Zhang, A. Sumi, M. Kimoto, Impact of El Nino on the East Asian monsoon: A diagnostic study of the '86/87 and '91/92 events. *J. Meteorol. Soc. Jpn.* **74**, 49-62 (1996).

28. M. Borga, M. Stoffel, L. Marchi, F. Marra, M. Jakob, Hydrogeomorphic response to extreme rainfall in headwater systems: Flash floods and debris flows. *J. Hydrol.* **518**, 194-205 (2014).

29. R. Lal, R. Francaviglia, *Sustainable Agriculture Reviews 29: Sustainable Soil Management: Preventive and Ameliorative Strategies*. (Springer, 2019), vol. 29, pp. 125-142.

30. W. Feng, L. Cheng, M. Cheng, Nondydrostatic numerical simulation for the "96.8" extraordinary rainstorm and the developing structure of mesoscale system. *Acta Meteorol. Sin.* **59**, 14 (2001).

31. Y. Ding, On the study of the unprecedented heavy rainfall in Henan Province during 4-8August 1975:Review and assessment. *Acta Meteorol. Sin.* **73**, 411-424 (2015).

32. R. Xing, Z. Ding, S. You, H. Xu, Relationship of tropical-cyclone-induced remote precipitation with tropical cyclones and the subtropical high. *Front. Earth Sci.* **10**, 595-606 (2016).

33. L. Chen, Y. Xu, Review of typhoon very heavy rainfall in China. *Meteorological Environmental Sciences* **40**, 3-10 (2017).

34. J. Yin *et al.*, A possible dynamic mechanism for rapid production of the extreme hourly rainfall in Zhengzhou City on 20 July 2021. *J. Meteorol. Res.* **36(1)**, 6-25 (2021).

35. Y. Nie, J. Sun, Moisture Sources and Transport for Extreme Precipitation Over Henan in July 2021. *Geophys. Res. Lett.* **49**, (2022).

36. Q. Xiao, L. Chen, X. Zhang, Evaluations of BDA Scheme Using the Advanced Research WRF (ARW) Model. *J. Appl. Meteorol. Climatol.* **48**, 680-689 (2009).

37. J. D. Woodruff, K. Kanamaru, S. Kundu, T. L. Cook, Depositional evidence for the Kamikaze typhoons and links to changes in typhoon climatology. *Geology* **43**, 91-94 (2015).

38. C. Ladlow, J. D. Woodruff, T. L. Cook, H. Baranes, K. Kanamaru, A fluvially derived flood deposit dating to the Kamikaze typhoons near Nagasaki, Japan. *Nat. Hazards* **99**, 827-841 (2019).

39. J. Zheng, W.-C. Wang, Q. Ge, Z. Man, P. Zhang, Precipitation variability and extreme events in eastern China during the past 1500 years. *Terr. Atmos. Ocean. Sci.* **17**, 579-592 (2006).

40. J. Chen, X. Zeng, Archaeological survey and inspecting excavation of the outer rammed earth wall foundation in Zhengzhou Shang City. *Cultural Relics of Central China* **1**, 89-97 (1991). (in Chinese)

41. Y. Liu, D. Zhang, The study on the Late Shang Culture in Zhengzhou area. *Kaogu (Archaeology)* **8**, 91-100 (2017). (in Chinese)

42. A. Song, Analysis of settlement patterns from prehistory to Shang and Zhou Period in Zhengzhou area. *East Asia Archaeology*, 156-194 (2011). (in Chinese)

43. X. Zhang, *Study on the Water Conservancy of the Shang Dynasty*. (China Social Science Press, Beijing, 2015), pp. 179-264. (in Chinese)

44. Y. He, Huanbei Shang City and Yinxu waterway systems and related issues. *Kaogu (Archaeology)* **9**, 82-94 (2021). (in Chinese)

45. W. Gu, The Neolithic site at Shuanghuaishu in Gongyi city, Henan. *Kaogu (Archeaology)* **7**, 27-48 (2021). (in Chinese)

46. P. J. Webster, G. J. Holland, J. A. Curry, H. R. Chang, Changes in tropical cyclone number, duration, and intensity in a warming environment. *Science* **309**, 1844-1846 (2005).

47. X. Wang, D. Jiang, X. Lang, Future extreme climate changes linked to global warming intensity. *Sci. Bull.* **62**, 1673-1680 (2017).

48. W. Cai *et al.*, ENSO and greenhouse warming. *Nat. Clim. Chang.* **5**, 849-859 (2015).

49. W. Mei, S.-P. Xie, F. Primeau, J. C. McWilliams, C. Pasquero, Northwestern Pacific typhoon intensity controlled by changes in ocean temperatures. *Sci. Adv.* **1**, e1500014 (2015).

Acknowledgments: This study was supported by Collaborative Innovation Centre for Climate Change via the 2011 program of Jiangsu Province, Research Funds for the Frontiers Science

Centre for Critical Earth Material Cycling (14380190, 14380187) of Nanjing University, and Social Science Foundation of Jiangsu Province, China (20LSC008). We thank Prof. Jon Woodruff at University of Massachusetts for providing the typhoon induced deposition data, and Profs. X. D. Tang and X. Qiu at Nanjing University for their suggestions in the typhoon simulations. We thank B. Zhu at Hunan Normal University, Z. Tao at the Institute of Geographic Sciences and Natural Resources Research in Chinese Academy of Sciences, and Y. Ma at Nanjing University for their help in data collection.

Data and materials availability: The meteorological data is from ERA5 and ERA5_land, which can be download in https://www.ecmwf.int/en/forecasts/datasets/reanalysis-datasets/era5. The typhoon tracks data is from https://tcdata.typhoon.org.cn/zjljsjj_zlhq.html. The satellite precipitation data is from Integrated Multi-satellite Retrievals for GPM (IMERG), which is available in https://gpm.nasa.gov/data/imerg. Data processing technique are available on request of corresponding author. The source code of the WRF model is available from http://www2.mmm.ucar.edu/wrf/users/download.

Supplementary Materials

Materials and Methods

Retrieving the drought, flood and rainfall indexes in the Late Shang dynasty

The database from which we obtained the three indexes (drought, flood and rainfall) comprised ~55000 pieces of oracle bone script divinations from the Late Shang dynasty. These pieces were retrieved from the most authoritative collections and studies of oracle bone scripts, including annotations or interpretations (Table S2).

The three drought, flood and rainfall indexes were derived from the three proportions of divinations containing the scripts for "pray for rain", "flood" and "rainfall condition" across the five oracle bone script phases. In contrast to floods and heavy rainfall events, droughts tend to have long-term statuses lasting months or even years, and this tendency results in an insufficient number of "drought" divinations for statistical significance. Therefore, we utilized the proportions of divinations that contained "pray for rain" instead of "drought" to build the drought condition index because "pray for rain" represents a more immediate response to a lack of rainfall and was included in the divinations much more frequently than the "drought" script.

The proportions of "locust-like" divinations were counted from an authoritative oracle bone script collection work by Yao & Xiao (*22*). In addition, although the water-wave-like pattern of the "disaster" character implies considerable disastrous effects of floods at that time, counting the proportions of this character did not lend statistical significance, as a "disaster" could refer to any natural or anthropogenic disaster, even disease.

Determining the impacts of typhoons on rainfall

Typhoons can lead to rainfall on the central plains of China directly (if a typhoon lands inland) or contribute to rainfall indirectly (by providing favorable moisture conditions). Therefore, we considered a rainfall event to be a typhoon-influenced one if an accompanying typhoon passed through the south-eastern seas of China (8°N to 38°N, 105°E to 140°E) on the same day the rainfall was recorded. And we define a northward typhoon-influenced rainfall event in this work if the typhoon reaches north of 28°N in its path. The distribution ranges of typhoons were determined according to multiple typical cases in which typhoons have caused extreme rainfall on the central plains of China (*32, 33*).

Impacts of non-landing typhoons on extreme rainfall near Zhengzhou and Anyang

To quantitatively understand the effects of non-landing typhoons on rainfall on the central plains of China, we performed two parallel numerical experiments representing each case using the Weather Research and Forecasting (WRF) model (*36*). (1) A Regular simulation (EXP_raw_typhoon) was conducted with the meteorological field initialized by European Centre for Medium-Range Weather Forecasts (ECMWF) ReAnalysis version 5 (ERA5) data one day before the cases shown in Fig. S5, D-F and was run for 72 hours. (2) An idealized numerical simulation, similar to the EXP_raw_typhoon simulation, was run; in this simulation, the typhoon intensity in the initial meteorological fields was reduced by half (by halving the maximum wind speed of Typhoons Therese, Kirogi and In-Fa) using Bogus (EXP_weak_typhoon) (*36*). When the typhoon intensities were reduced, rainfall near Zhengzhou and Anyang decreased significantly (Fig. S6), suggesting that these typhoons contributed to extreme rainfall. This finding agrees with the results of previous studies (*30, 33-35*). The applied modelling settings are shown in Table S5.

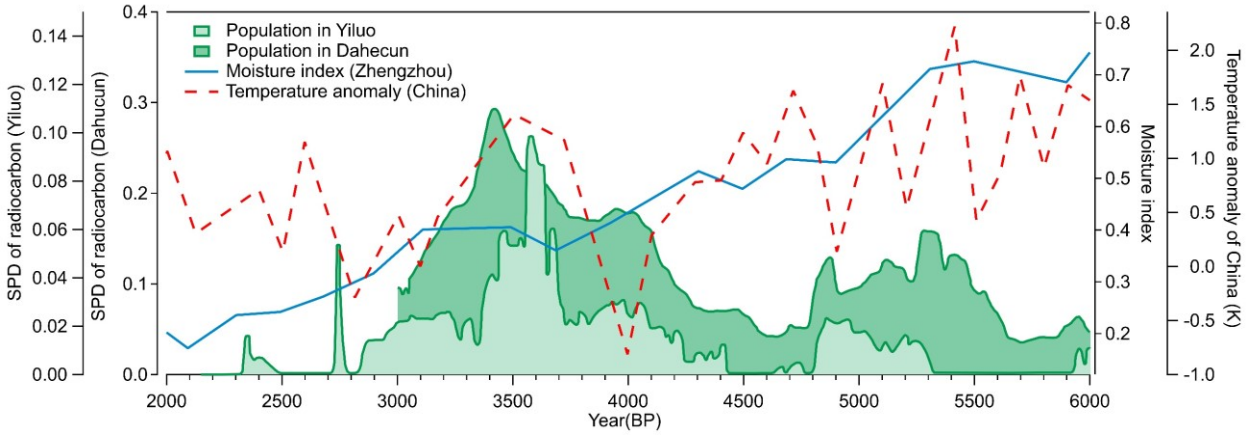

Fig. S1. Variation of population size (represented by SPD of radiocarbon) in the Yiluo region and at the Dahecun site with corresponding time series of several meteorological elements. Temperature anomaly of China (*18*) and the moisture index around Zhengzhou (*17*).

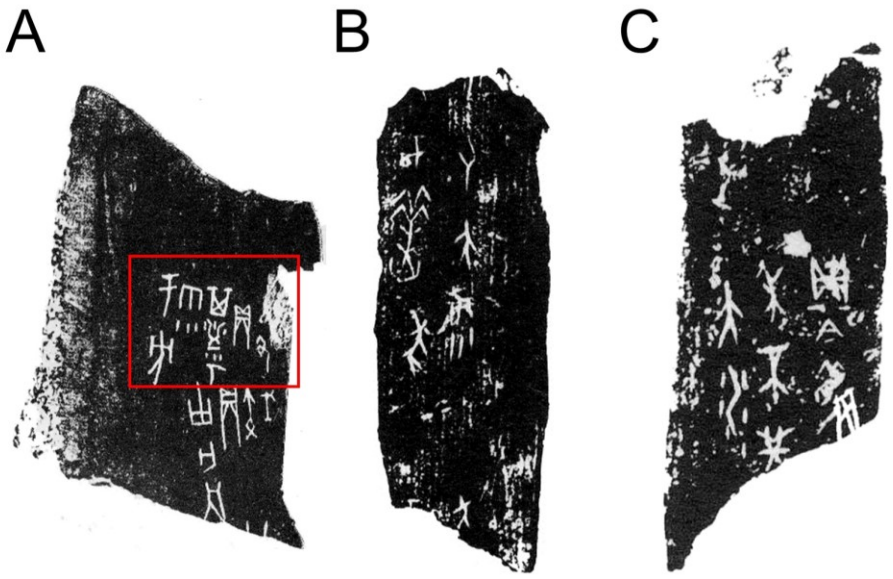

Fig. S2. Typical rubbing examples that contain "rain", "praying for rain" and "flood" (from *Oracle Bone Script Complications*, Table S2). (**A**) Piece No. 32992, "Divination in the day of Dingchou: Will the god of Fang get rid of the heavy rains?" The interpretation is for the inscriptions in the red box. (**B**) Piece No. 34226, "Shall we pray to the mountain god for rain?" (**C**) Piece No. 33351, "Will there be a flood that threatens the millet harvest this autumn?"

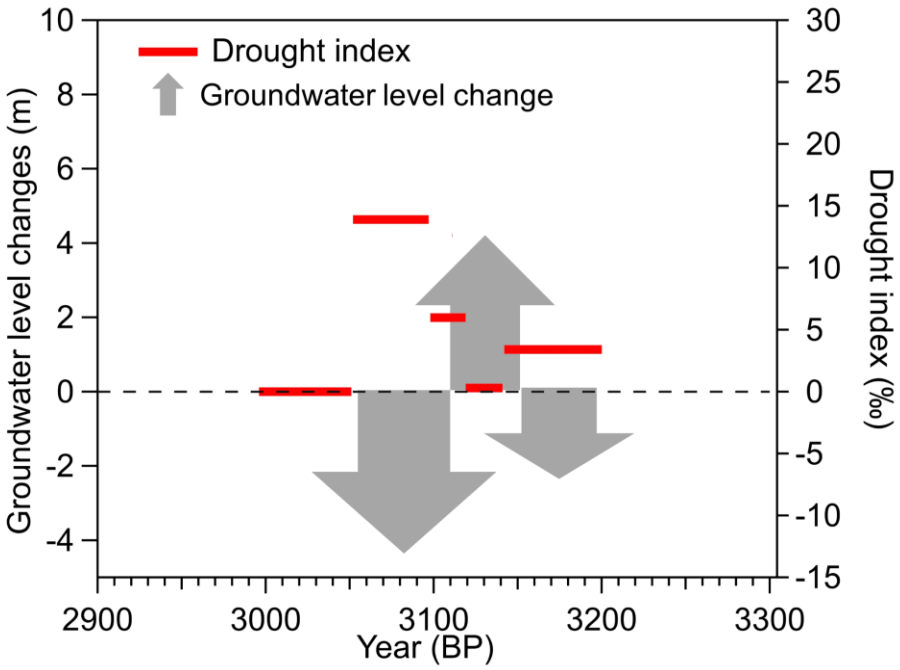

Fig. S3. Comparison of the drought index and the groundwater level changes in Late Shang. The width of each arrow (tail) shows a time to which the age of certain groundwater level data belongs (*23*).

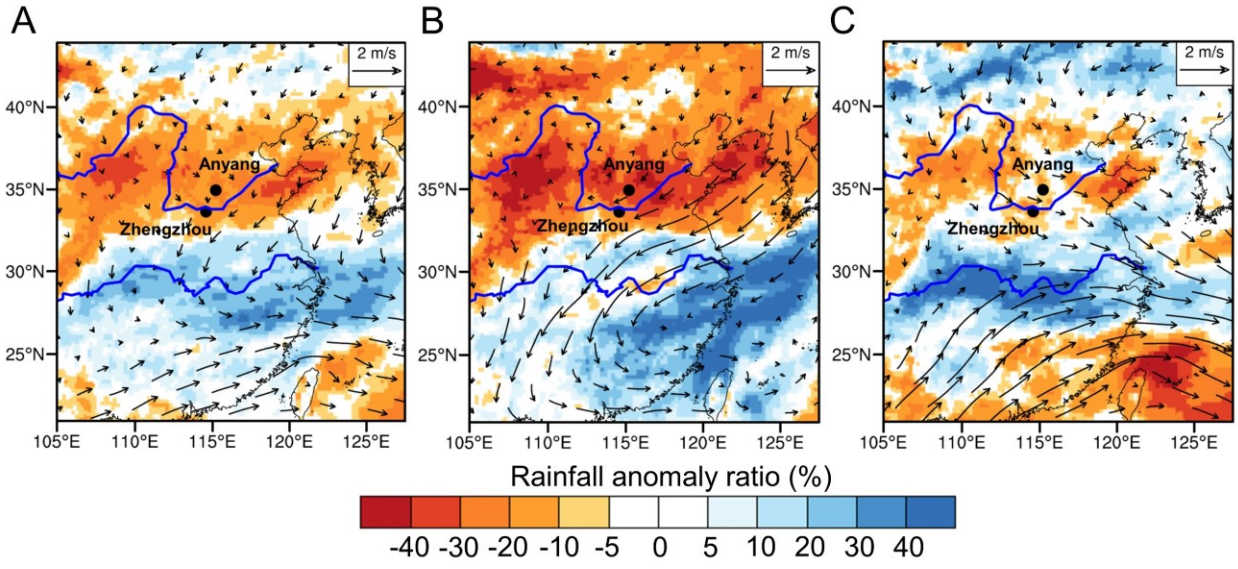

Fig. S4. The impacts of strong El Niño events on summer rainfall in China. (**A**) Rainfall anomaly ratio in strong El Niño years (1982-1983, 1997-1998, 2015-2016) compared to the average (1950-2021). (**B-C**) Similar to (A) but for El Niño developing and decaying years respectively. The vectors give the wind field anomaly at 850 hPa.

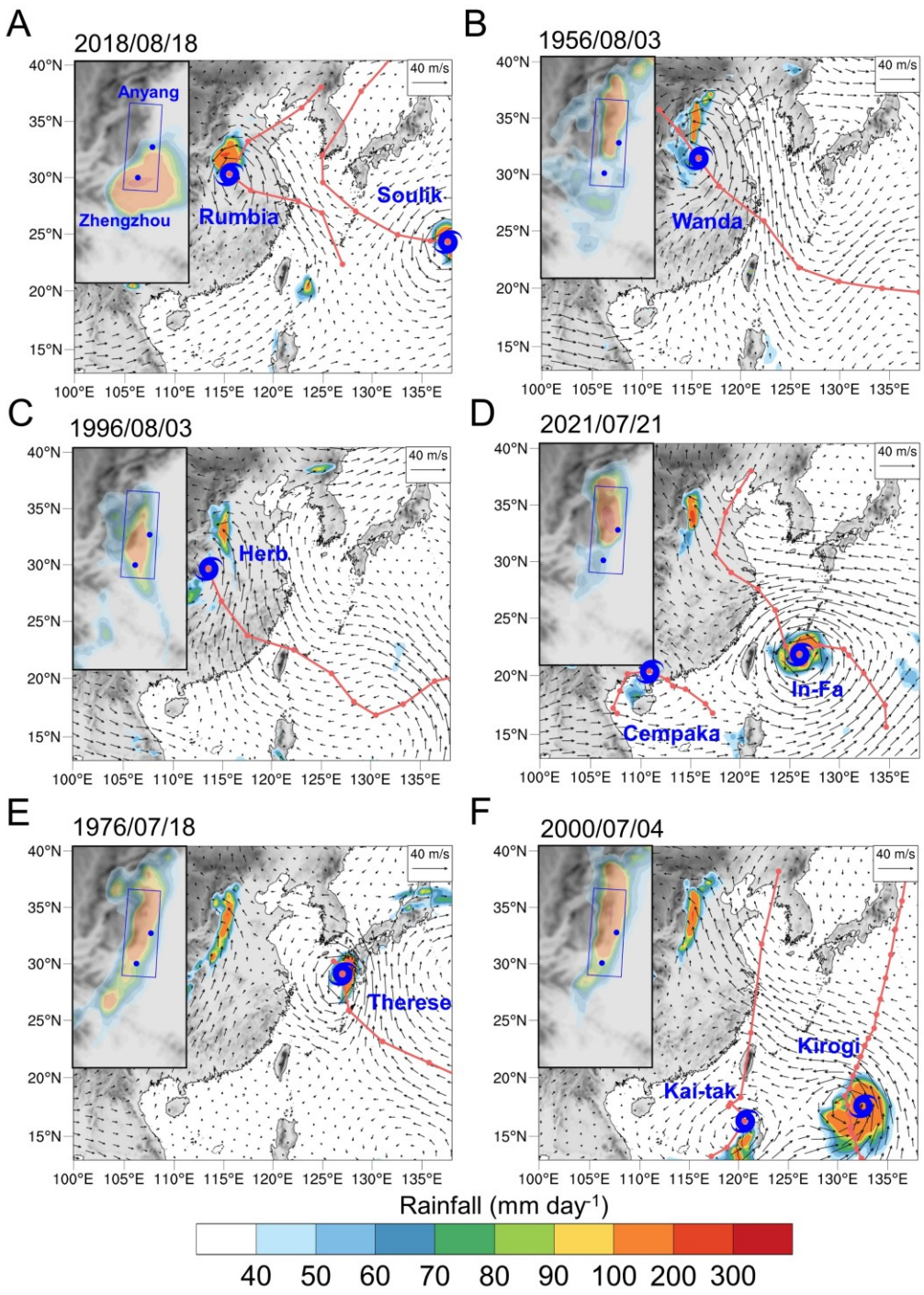

Fig. S5. Representative typhoon influenced rainfall cases in Zhengzhou, Anyang and the surrounding area. (**A-F**) Typhoons contribute to 7 out of the 8 largest daily precipitation cases in Zhengzhou and Anyang area, 1950-2021. We present 6 typhoon influenced cases here as two cases share a same typhoon process. The 6 cases are presented in an increasing order. Red lines give the track of typhoons with the markers indicate typhoon center locations at 12 UTC every day. The small picture in every upper left corner is an enlarged view of rainfall on the central plains of China. Severe flood disasters have been caused by the heavy rains in all cases.

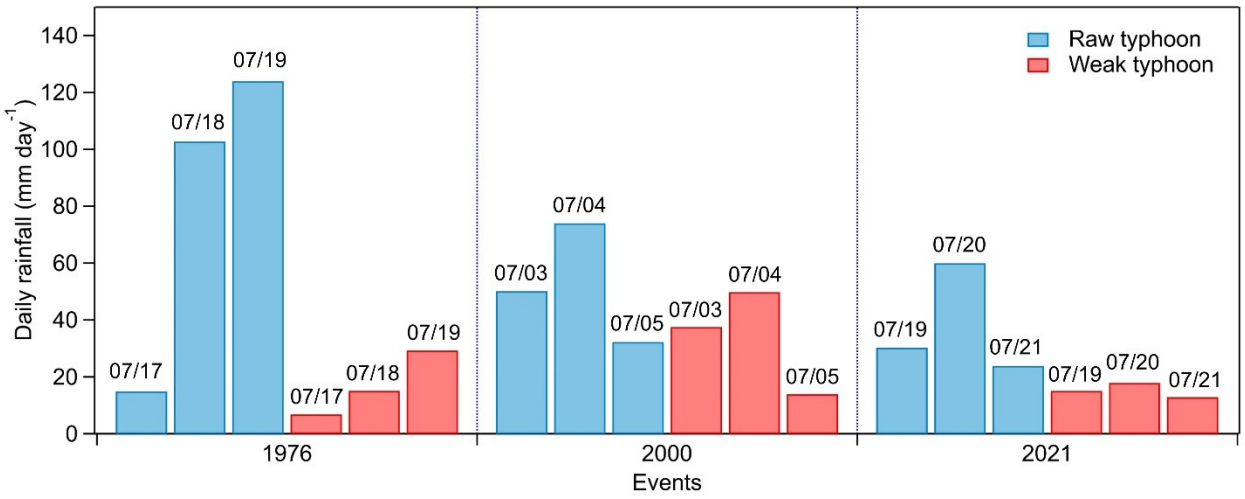

Fig. S6. Simulated rainfall near Zhengzhou and Anyang under raw and weak typhoon conditions. The cases in 1976, 2000 and 2021 corresponds to the cases in Fig. S5, D-F. The numbers above the bars show the date of the rainfall.

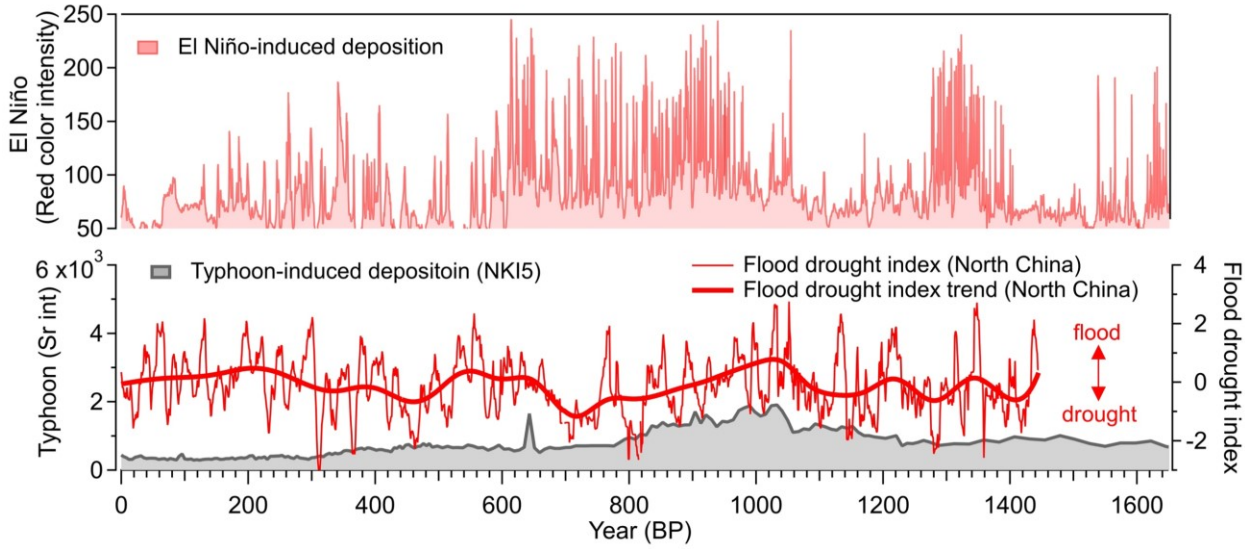

Fig. S7. Impacts of El Niño and typhoons on the floods or droughts in North China in the millennial scale. Variation of flood and drought situations (represented by flood drought index (*39*)) from 1650 BP along with the corresponding variations of El Niño (*19*) and typhoon *(20)*. The flood/drought is heavier when flood drought index is positive/negative. The trend of the flood drought index is calculated by 100-year EEMD filter smoothing.

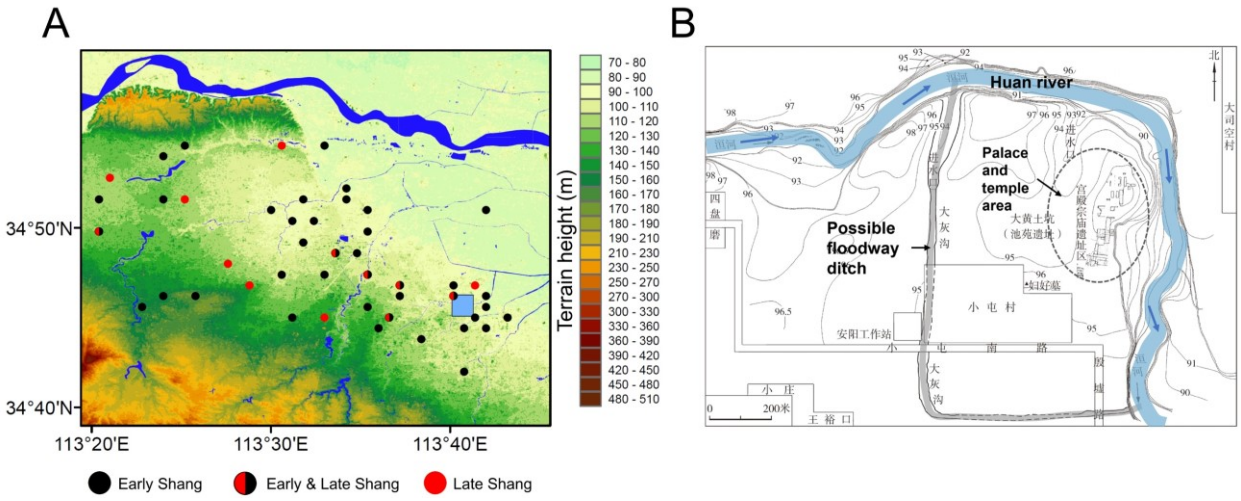

Fig. S8. Archaeological evidences of the impacts of flood disasters in the Shang dynasty. (**A**) Change in the settlement siting preferences: lower course of rivers in the Early Shang dynasty, middle and upper course of rivers in the Late Shang dynasty (*41, 42*). The dark blue lines give the locations of rivers in nowadays. The light blue box is the location of Zhengzhou Shang city, which belongs to early Shang. (**B**) Layout of the Palace area of Yinxu site in Late Shang dynasty with the blue wide stripe showing the Huan river and the grey narrow stripe showing a possible floodway ditch (*43, 44*).

Table S1. Periods defining and the time span

Period number	Periods	Specific phases of archaeological cultures / Dynasties	Locations of cultural and civilization centers in central China	Time span
1	Middle Yangshao	Miaodigou phase of Yangshao culture	Sanmenxia and nearby areas	5950-5050 BP
2	Late Yangshao	Qinwangzhai phase of Yangshao culture	Zhengzhou, Luoyang and nearby areas	5650-4650 BP
3	Early Longshan	Miaodigou Ⅱ phase of Longshan culture in Henan	Sanmenxia and nearby areas	4850-4550 BP
4	Late Longshan	Wangwan Ⅲ phase of Longshan culture in Henan	Zhengzhou, Luoyang and nearby areas	4550-3800 BP
5	Xinzhai - Erlitou	Xia Dynasty to Shang Dynasty	Zhengzhou, Luoyang and nearby areas	3800-3470 BP
6	Early Shang	Shang Dynasty	Zhengzhou, Luoyang and nearby areas	3550-3250 BP
7	Late Shang	Shang Dynasty	Anyang and nearby areas	3250-2946 BP

Table S2. Oracle bone scripts data source

Oracle bone script data source (translation)	Oracle bone script data source in Chinese
Guo, M. *et al*. *Oracle Bone Script Complications (1-13)*. (China Book Company, 1978-1983). (in Chinese)	郭沫若主编，胡厚宣总编辑，中国社会科学院历史研究所编辑:《甲骨文合集》(1-13)，北京：中华书局，1978-1983年。
Hu, H. *Interpretation of Oracle Bone Script Complications (1-4)*. (China Social Science Press, 1999). (in Chinese)	胡厚宣主编:《甲骨文合集释文》(1-4)，北京：中国社会科学出版社，2009 年。
The Institute of Archaeology, C. A. o. S. S. *The Oracle Bones at South Xiaotun Site, Volume One (1-2)*. (China Book Company, 1980). (in Chinese)	中国社会科学院考古研究所编著:《小屯南地甲骨(上册)》(1-2)，北京：中华书局，1980 年。
The Institute of Archaeology, C. A. o. S. S. *The Oracle Bones at South Xiaotun Site, Volume Two (1-3)*. (Zhonghua Book Company, 1984). (in Chinese)	中国社会科学院考古研究所编著:《小屯南地甲骨(下册)》(1-3)，北京：中华书局，1984 年。
Yao, X. & Xiao, D. *Textual Research of Oracle Bones at South Xiaotun Site*. (China Book Company, 1985). (in Chinese)	姚孝遂、肖丁:《小屯南地甲骨考释》，北京：中华书局，1985 年。
Li, X., Qi, W. & Ai, L. *Oracle Bone Collections in Great Britain, Volume One (1-2)*. (China Book Company, 1985). (in Chinese)	李学勤、齐文心、艾兰编著:《英国所藏甲骨集（上编)》(上、下)，北京：中华书局，1985 年。
Li, X., Qi, W. & Ai, L. *Oracle Bone Collections in Great Britain, Volume Two (1-2)*. (China Book Company, 1985). (in Chinese)	李学勤、齐文心、艾兰编著:《英国所藏甲骨集（下编)》(上、下)，北京：中华书局，1992 年。
Peng, B., Xie, J. & Ma, J. *Supplement to Oracle Bone Script Complications (1-7)*. (Lauguage & Culture Press, 1999). (in Chinese)	彭邦炯、谢济、马季凡编著:《甲骨文合集补编》(1-7)，北京：语文出版社，1999 年。
The Institute of Archaeology, C. A. o. S. S. *The Oracle Bones at East Huanyuanzhuang Site in Yinxu (1-6)*. (Yunnan People's Publishing House, 2003). (in Chinese)	中国社会科学院考古研究所编著:《殷墟花园庄东地甲骨》(1-6)，昆明：云南人民出版社，2003 年。

Table S3. Phases of oracle bone scripts and the time span

Phase number	Phases (shown as name(s) of the king(s))	Time span
1	Wuding (武丁 in Chinese)	3200-3142 BP
2	Zugeng, Zujia (祖庚，祖甲 in Chinese)	3141-3098 BP
3	Linxin, Kangding (廩辛，康丁 in Chinese)	
4	Wuyi, Wending (武乙，文丁 in Chinese)	3097-3052 BP
5	Diyi, Dixin (帝乙，帝辛 in Chinese)	3051-2996 BP

According to the age-dating of the five phases of oracle bone scripts, phases 2 to 3 are around 3141–3098 BP. We roughly divide this timespan into two equal parts.

Table S4. Quantitative analyses of oracle bone scripts in the five phases

Phase number	Total count (pieces)	Containing “rainfall” (count, proportion)	Containing “pray for rain” (count, proportion)	Containing “flood” (count, proportion)
1	29061	2450 (8.43%)	99 (3.41‰)	32 (1.11‰)
2	6616	423 (6.39%)	2 (0.03 ‰)	4 (0.61‰)
3	7855	1175 (14.96%)	47 (5.98‰)	3 (0.38‰)
4	5341	709 (13.27%)	74 (13.86‰)	18 (3.37‰)
5	6600	126 (1.91%)	0 (0.00‰)	1 (0.15‰)

Table S5. Model configuration options and settings

Domain setting	
Horizontal grid	280 × 300
Grid spacing	20 km × 20 km
Vertical layers	31 eta levels
Centre point	120 ^{o}E, 30 ^{o}N
Map projection	Lambert
Paramerization configuration	
Long-wave radiation	Dudhia scheme
Short-wave radiation	Dudhia scheme
Cumulus parameterization	Kain-Fritsch
Land-surface	Noah
PBL	YSU
Microphysics	WRF Single-Moment 3-class scheme